Acta Crystallographica Section D
Biological Crystallography
ISSN 0907-4449

Design of specific peptide inhibitors of phospholipase A_2: structure of a complex formed between Russell's viper phospholipase A_2 and a designed peptide Leu-Ala-Ile-Tyr-Ser (LAIYS)

Vikas Chandra,[a] Jayasankar Jasti,[a] Punit Kaur,[a] Sharmistha Dey,[a] A. Srinivasan,[a] Ch. Betzel[b] and T. P. Singh[a]*

[a]Department of Biophysics, All India Institute of Medical Sciences, New Delhi 110029, India, and [b]Institute of Medical Biochemistry and Molecular Biology, UKE c/o DESY, Notkestrasse 85, 22603 Hamburg, Germany

Correspondence e-mail: tps@aiims.aiims.ac.in

Received 17 April 2002
Accepted 30 July 2002

PDB Reference: PLA_2–LAIYS, 1jq8.

Phospholipase A_2 (EC 3.1.1.4) is a key enzyme of the cascade mechanism involved in the production of proinflammatory compounds known as eicosanoids. The binding of phospholipase A_2 to membrane surfaces and the hydrolysis of phospholipids are thought to involve the formation of a hydrophobic channel into which a single substrate molecule diffuses before cleavage. In order to regulate the production of proinflammatory compounds, a specific peptide inhibitor of PLA_2, Leu-Ala-Ile-Tyr-Ser, has been designed. Phospholipase A_2 from *Daboia russelli pulchella* ($DPLA_2$) and peptide Leu-Ala-Ile-Tyr-Ser (LAIYS) have been co-crystallized. The structure of the complex has been determined and refined to 2.0 Å resolution. The structure contains two crystallographically independent molecules of $DPLA_2$, with one molecule of peptide specifically bound to one of them. The overall conformations of the two molecules are essentially similar except in three regions; namely, the calcium-binding loop including Trp31 (residues 25–34), the β-wing consisting of two antiparallel β-strands (residues 74–85) and the C-terminal region (residues 119–133). Of these, the most striking difference pertains to the orientation of Trp31 in the two molecules. The conformation of Trp31 in molecule *A* was suitable to allow the binding of peptide LAIYS, while that in molecule *B* prevented the entry of the ligand into the hydrophobic channel. The structure of the complex clearly showed that the OH group of Tyr of the inhibitor formed hydrogen bonds with both His48 $N^{\delta1}$ and Asp49 $O^{\delta1}$, while $O^{\gamma}H$ of Ser was involved in a hydrogen bond with Trp31. Other peptide backbone atoms interact with protein through water molecules, while Leu, Ala and Ile form strong hydrophobic interactions with the residues of the hydrophobic channel.

1. Introduction

Phospholipases A_2 (PLA_2s; EC 3.1.1.4) represent a class of enzymes that catalyze the hydrolysis of membrane phospholipids to release free fatty acids. In particular, they hydrolyze the *sn*-2 acyl bond of phospholipids, producing equimolar amounts of lysophospholipids and free fatty acids. The ability of PLA_2s to produce substrates for the generation of inflammatory lipid mediators in the process of tissue injury and rheumatoid arthritis (Wery *et al.*, 1991) makes this specific class of phospholipases very important targets for the design of specific drugs against inflammation. We have previously reported complexes of phospholipase A_2 with vitamin E (Chandra *et al.*, 2002*a*) and aristolochic acid (Chandra *et al.*, 2002*b*) in which OH groups from these inhibitors formed hydrogen bonds with Asp49 $O^{\delta1}$ and His48 $N^{\delta1}$ simulta-

© 2002 International Union of Crystallography
Printed in Denmark – all rights reserved

neously. In addition to these key interactions, the natural inhibitors were involved in a number of other attractive hydrophobic interactions. Using these observations as a guiding principle, a pentapeptide Leu-Ala-Ile-Tyr-Ser (LAIYS) was designed to inhibit the function of PLA_2. Kinetic studies have indicated an improved value of K_i over the two previously reported natural inhibitors vitamin E (K_i = 1.6 ± 0.1 μ*M*; Chandra *et al.*, 2002*a*) and aristolochic acid (K_i = 1.2 ± 0.1 μ*M*; Chandra *et al.*, 2002*b*). In order to further design peptides with enhanced binding affinities, it is necessary to determine the interactions of the peptide LAIYS with PLA_2. Therefore, a complex between PLA_2 from *D. russelli pulchella* ($DPLA_2$) and the designed peptide LAIYS was co-crystallized and the detailed three-dimensional structure was determined. Here, we report the results of a detailed structure analysis of the complex.

2. Experimental procedures

2.1. Purification of $DPLA_2$

$DPLA_2$ was purified from crude venom obtained from Irula Snake Catchers Industrial Society Limited, Chennai, India. The purification procedure was developed in our laboratory as reported previously (Chandra *et al.*, 1999). It involves an affinity step on Cibacron blue matrix and ion-exchange chromatography on CM Sephadex C-25.

2.2. Synthesis of LAIYS

The peptide was synthesized using a PS3 automated solid-phase peptide synthesizer (Rainin, USA). The resin used was Fmoc-Ser-Wang resin and the solvent used for synthesis was dimethylformamide (DMF).

In the first step, Fmoc-Ser-Wang resin (1 g, 0.5 m*M*) was deprotected by 20% piperidine in DMF to form H_2N-Ser-Wang resin. The uronium salt 2-(1*H*-benzotriazole-1-yl)-1,1,3,3-tetramethyl uronium hexafluorophosphate (HBTU) (455 mg; 1 m*M*) in the presence of the base *N*-methylmorpholine (NMM; 0.4 *M*) activated the amino acid to form the active ester of Fmoc-Tyr-OH (551 mg; 0.5 m*M*). This was coupled with H_2N-Lys-Wang resin to obtain Fmoc-Tyr-Ser-Wang resin. The above procedure was repeated for the remaining amino acids until the complete sequence Fmoc-Leu-Ala-Ile-Tyr-Ser-Wang resin was formed. The resin was cleaved with trifluoroacetic acid (TFA). The peptide was purified by reverse-phase chromatography on C_{18} PepRPC column (1.6 × 1.0 cm, Pharmacia, Hong Kong). The purity of the peptide was confirmed by determining its primary sequence with a PPSQ-21A protein sequencer (Shimadzu, Japan).

2.3. Kinetic and inhibition studies of $DPLA_2$ by peptide LAIYS

The purified enzyme was used for kinetic studies. In order to determine the inhibitory potency of the designed peptide LAIYS, the value of its inhibitor constant (K_i) was estimated. In the kinetic experiments, the 1,2-dithio analogue of diheptanoyl phosphatidylcholine was used as a substrate (PLA_2 assay kit, Cayman Chemicals, Michigan, USA). Upon hydrolysis of the thio-ester bond at the *sn*-2 position by PLA_2, free thiols were liberated which were detected using 5,5′-dithiobis-(2-nitrobenzoic acid) (DTNB). All assays were performed in 20 m*M* sodium cacodylate buffer pH 7.0 at 298 K. The enzyme concentrations were fixed at 1.5 m*M*, while substrate concentrations were varied from 0.5 to 2.0 m*M*. PLA_2 was incubated separately with 0.5, 1.0 and 1.5 μ*M* concentrations of LAIYS for 30 min. The reactions were initiated by addition of 0.5, 0.7, 1.0, 1.4 and 2.0 m*M* of substrates for each inhibitor concentration and the resulting products were estimated by the differences in absorbance at 414 nm. In separate experiments, the inhibitory assays with 1:1, 1:10 and 1:20 molar ratios of enzyme and designed peptide LAIYS were also carried out.

2.4. Dynamic light scattering (DLS)

As reported previously (Chandra *et al.*, 2001), two molecules of $DPLA_2$ were found to be strongly associated in both crystalline and solution states even at very low concentrations. However, every new preparation of $DPLA_2$ was examined for molecular association using the DLS system (Dlerks & Partner, Hamburg, Germany) and analyzed using the software described by Schulze (1996). The sample solutions were prepared in sodium cacodylate buffer (20 m*M*, pH 6.5) made with de-ionized water from a Millipore Alpha-Q system. The samples were filtered through 0.1 μm polyvinylidene difluoride filters (Millipore). The enzyme concentrations were varied from 0.05 to 20 mg ml^{-1} at a constant temperature of 298 K. Samples were manually injected into the flow cell (50 μl) and illuminated by a 25 mW, 600 nm solid-state laser. Data were collected in quintuplicate for each measurement.

2.5. Crystallization

Purified samples of $DPLA_2$ were dissolved in 1 m*M* $CaCl_2$, 3% dioxane, 20 m*M* sodium cacodylate buffer pH 6.5 to a final protein concentration of 15 mg ml^{-1}. Peptide LAIYS was then added in higher molar concentrations. This mixture of protein and the peptide LAIYS was allowed to stand in the vials for 24 h; 25 μl drops of the above mixture were then equilibrated using the sitting-drop vapour-diffusion method against 1.4 *M* ammonium sulfate in the same buffer containing 3% dioxane. Rectangular-shaped colourless crystals of dimensions up to 0.5 × 0.4 × 0.3 mm were obtained at 298 K within two weeks.

2.6. Data collection

The crystals of the complex were stabilized in 15% glycerol as a cryoprotectant for data collection at low temperature. A single crystal was mounted in a nylon loop and flash-frozen in a stream of nitrogen gas at 100 K. The data were collected on EMBL beamline X-11 at DESY, Hamburg, Germany with λ = 0.98 Å using a MAR 345 imaging-plate scanner. The data were processed using *DENZO* and *SCALEPACK* (Otwinowski & Minor, 1997). The results of the data collection and processing are given in Table 1.

2.7. Structure determination and refinement

The structure was obtained by the molecular-replacement method using the structure of $DPLA_2$ determined previously at 1.9 Å resolution (Chandra *et al.*, 2001). The structure contains two molecules of $DPLA_2$ in the asymmetric unit, designated molecules *A* and *B*. The refinement was carried out with the program *CNS* (Brünger *et al.*, 1998). In each step $2F_o - F_c$ and $F_o - F_c$ maps were calculated to improve the structure in the density maps using the program *O* (Jones *et al.*, 1991). The resolution was extended stepwise from 3.0 to 2.0 Å. Several cycles of positional refinement with restrained individual *B*-factor refinement and rounds of 3000 K simulated annealing allowed the correct tracing of flexible loops where the conformations were found to be different from the initial model. At the end of this stage, R_{cryst} fell to 0.224 and R_{free} was 0.268. Both Fourier ($2F_o - F_c$) and difference Fourier ($F_o - F_c$) maps computed at this stage clearly indicated the presence of the peptide in the binding site of molecule *A* (Fig. 1). However, there was no continuous density in the corresponding regions of molecule *B* and it was interpreted as three discrete water molecules. As this was an unexpected result, the $2F_o - F_c$ and $F_o - F_c$ maps were calculated at various cutoffs at different stages of refinement, which showed that the peptide was indeed not present in molecule *B*. These maps, however, showed clear electron densities for one sulfate and six acetate ions. There was no density for calcium ions even though 1 m*M* $CaCl_2$ was added to the protein solution for crystallization. A total of 285 water molecules were also located from the difference Fourier maps using a cutoff of 3σ. All these were included in subsequent rounds of refinement, including 3000 K simulated annealing. Details of the refinement and other parameters are listed in Table 2.

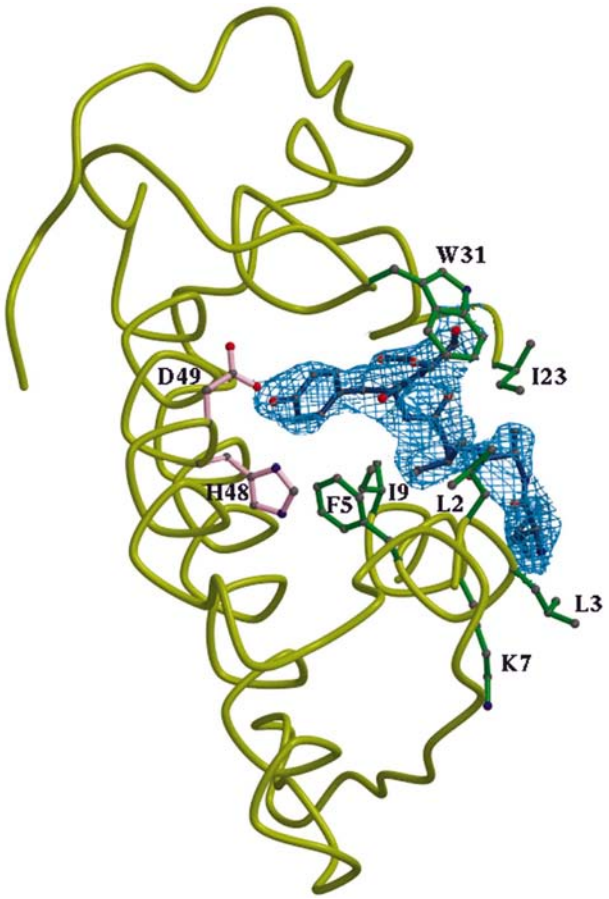

Figure 1
The $(F_o - F_c)$ map contoured at 2.5σ showing the electron density for the peptide LAIYS in molecule *A*.

Table 1
Crystallographic data for the complex formed between $DPLA_2$ and the pentapeptide LAIYS.

Values in parentheses are for the highest resolution shell.

Space group	$C222_1$
Unit-cell parameters (Å)	
a	76.82
b	90.38
c	77.59
V_M (Å^3 Da^{-1})	2.6
Solvent content (%)	53
Z	16
Resolution range (Å)	20.0–2.0 (2.07–2.0)
No. of observed reflections	222133
No. of unique reflections	17914
Completeness of data (%)	96.3 (88.1)
R_{sym} (%)	2.0 (9.7)
$I/\sigma(I)$	43.8 (2.5)

Table 2
Summary of crystallographic refinement.

PDB code	1jq8
Resolution limits (Å)	20.0–2.0
No. of reflections	17914
R_{cryst} (for all data) (%)	18.9
R_{free} (5% data) (%)	19.8
Protein atoms	1888
Pentapeptide (LAIYS) atoms	40
Sulfate ion	1
Acetate ions	6
Water molecules	285
R.m.s. deviations in bond lengths (Å)	0.006
R.m.s. deviations in bond angles (°)	1.3
R.m.s. deviations in dihedral angles (°)	22.6
Overall *G* factor	2.2
Average *B* factor for main-chain atoms (Å^2)	34.5
Average *B* factor for side-chain atoms and waters (Å^2)	42.1
Average *B* factor for all atoms (Å^2)	38.7
Residues in the most allowed regions (%)	90.4
Estimated coordinate error (after Luzzati, 1952) (Å)	0.20
Estimated coordinate error (from σ_A; Read, 1986) (Å)	0.22

3. Results and discussion

3.1. Quality of the model

The final model consists of two $DPLA_2$ molecules, one peptide molecule, one sulfate and six acetate ions and 285 water molecules. The dispersion precision indicator (Cruickshank, 1999; Murshudov & Dodson, 1997) estimates an average root-mean-square (r.m.s.) coordinate error of 0.15 Å. The overall *G* factor calculated by *PROCHECK* (Laskowski *et al.*, 1993, 1994) as a measure of stereochemical quality of the model is 2.2, which is somewhat better than expected at this resolution. 90.4% of the non-glycine residues fall in the most

favoured regions of the Ramachandran plot (Ramachandran & Sasisekaran, 1968).

3.2. Inhibition of PLA_2 by the peptide LAIYS

The purified samples of $DPLA_2$ showed a molecular weight of 14 kDa on SDS–PAGE (Chandra *et al.*, 1999). However, the results of dynamic light-scattering (DLS) experiments indicated a mean hydrodynamic radius (R_H) of 2.5 nm for $DPLA_2$ in the protein concentration range 0.05–20.0 mg ml^{-1}, which corresponds to a molecular weight of 28 kDa (Schmitz, 1990; Dahneke, 1983). Since the polydispersity value in these estimations was below 15% of the average radius, all $DPLA_2$ molecules in solution existed in the dimeric form. A careful estimation of the void volumes in the gel-filtration profile of $DPLA_2$ also suggested a molecular weight of 28 kDa.

The percentage inhibition values of $DPLA_2$ by peptide LAIYS at different molar ratios of 1:1, 1:10 and 1:20 of enzyme to peptide were estimated. Unexpectedly, at all these concentrations the levels of inhibition of $DPLA_2$ were found to be the same, showing 50% inhibition of the enzyme. Kinetic experiments carried out separately clearly showed that the peptide acted as a competitive inhibitor of $DPLA_2$, with a K_i value of $1.01 \pm 0.10\ \mu M$. The calculated K_M value for the substrate was found to be 0.72 ± 0.05 mM. Therefore, the high molar ratios of peptide to enzyme (10:1, 20:1) would be expected to show higher levels of inhibition. However, only 50% inhibition could be achieved, suggesting that the peptide could bind only to 50% of the $DPLA_2$ molecules. In the control experiments, $DPLA_2$ showed 100% activity where standard substrates were used without peptide inhibitor. This might be attributed to either having unsuitable conformations of the binding sites in 50% of the molecules towards the peptide inhibitor or the binding sites of 50% of the $DPLA_2$ molecules not being physically accessible to the peptide inhibitor. Both of these effects in $DPLA_2$ can be caused by the association of two molecules. Indeed, it has been shown by earlier studies (Chandra *et al.*, 2000, 2001) that the association of two molecules converts the binding site of molecule *A*, which is located at the interface, into a suitable form of conformation for the binding of ligands, but not the binding site of molecule *B*. These studies have also shown that the surface-exposed hydrophobic channel in molecule *B* seems to be completely uninfluenced by the association and hence the observed unsuitable conformation of the hydrophobic channel may be an inherent property of $DPLA_2$. Therefore, as in the previous studies (Chandra *et al.*, 2002*a*,*b*), the peptide inhibitor binds to molecule *A* despite the binding site being located at the interface and does not bind to molecule *B* even though the binding is exposed to the surface. The observation of 100% binding by naturally occurring substrates indicates that these are capable of dissociating the two molecules for binding to molecule *A* and are also able to induce a suitable conformation in molecule *B* for achieving full activity of $DPLA_2$.

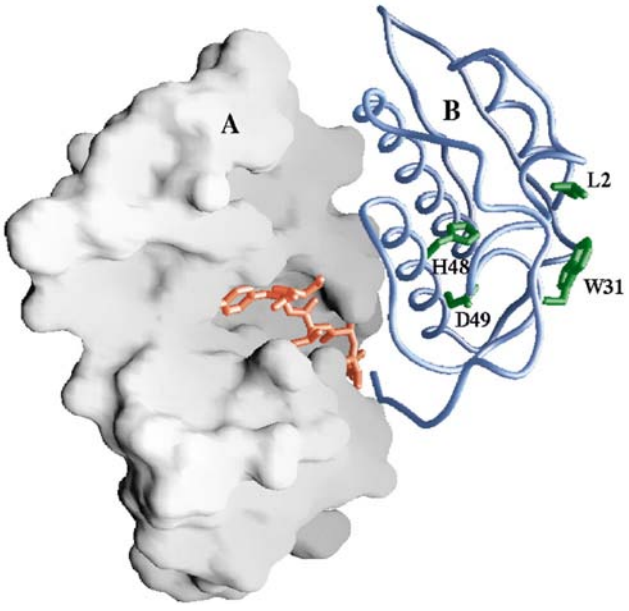

Figure 2
The association of molecules *A* and *B* showing the long interface. The opening of the hydrophobic channel of molecule *A* is located at the interface, while that of molecule *B* is situated at the surface. Molecule *A* is shown in surface representation with the peptide (red) in the binding channel and molecule *B* is drawn in backbone mode. The hydrophobic channel in molecule *B* opens to the surface at Trp31 and Leu2.

3.3. Molecular associations

The structure contains two crystallographically independent molecules *A* and *B*. The gel-filtration profile and DLS studies have indicated that the two molecules are also associated in solution. The structure shows that the long interface between the two molecules is stabilized by several hydrogen bonds and a number of hydrophobic interactions. The entrance to the hydrophobic channel of molecule *A* opens to the interface created by the association of molecules *A* and *B*, while that of *B* lies at the outer surface of the associated unit (Fig. 2). The overall conformations of molecules *A* and *B* are found to be essentially similar. The superposition of molecules *A* on *B* shows an r.m.s. displacement of 0.76 Å for the C^{α} positions. A plot of the r.m.s. displacements between C^{α} positions of

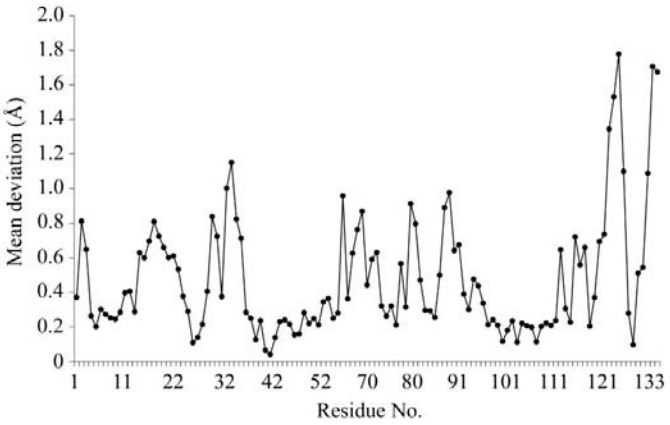

Figure 3
Plot of mean deviations between C^{α} traces of molecules *A* and *B* *versus* residue number.

molecules *A* and *B* against residue number is shown in Fig. 3. There are three prominent regions which show strong differences in the conformations of the two molecules, namely (i) the calcium-binding loop including Trp31 (residues 25–34), the β-wing consisting of two antiparallel β-strands (residues 74–85) and the C-terminal residues 119–133. These regions are functionally relevant, with a particular reference to the calcium-binding loop which is intimately linked to the resulting conformation of the hydrophobic channel. It may be noted that Trp31 forms a lid to the hydrophobic channel and its orientation undergoes changes in order to close and open the gate to the channel.

3.4. Binding of LAIYS to $DPLA_2$

The electron density for LAIYS in molecule *A* is exceptionally clear, allowing a detailed description of the interactions between $DPLA_2$ and the peptide LAIYS. In contrast, the corresponding region in molecule *B* is completely empty. This shows that molecule *A* adopts a conformation that is

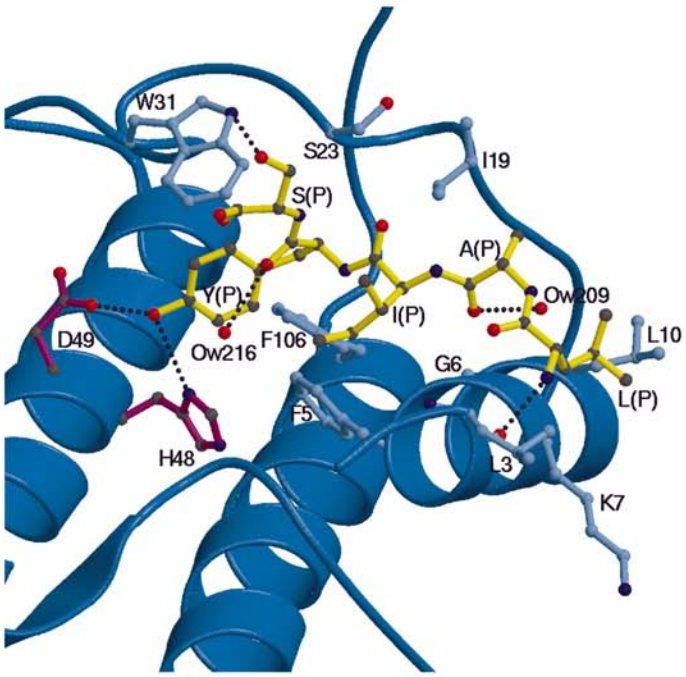

(*a*)

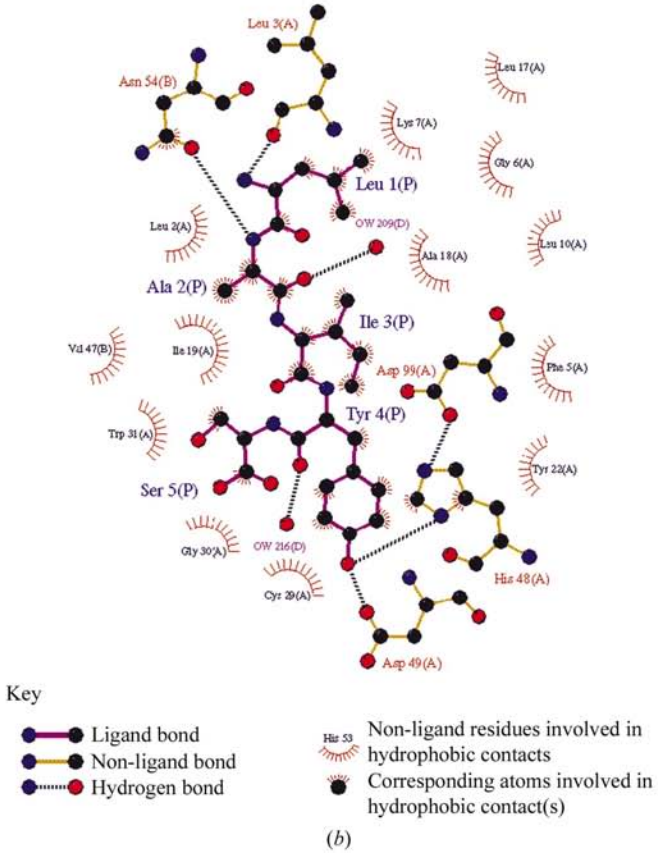

(*b*)

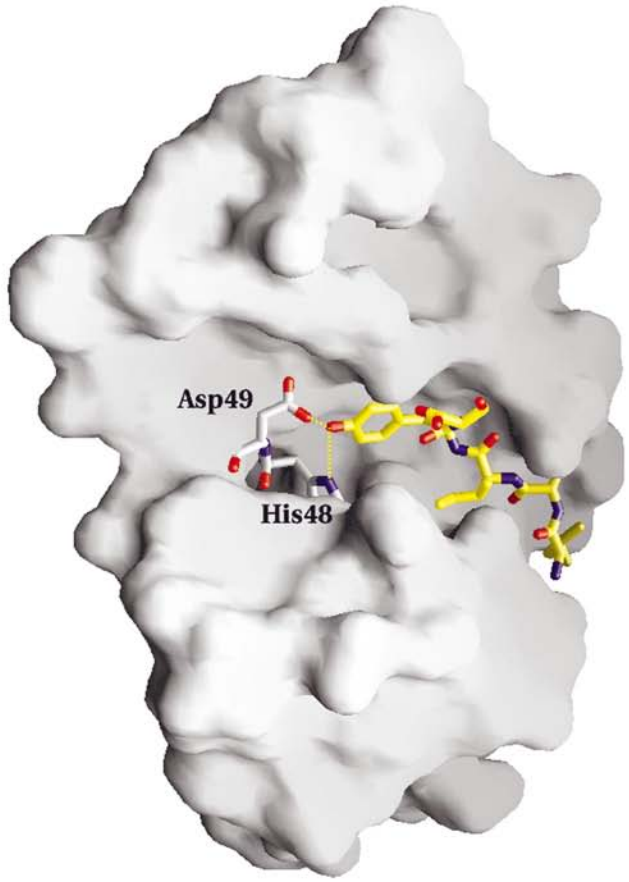

(*c*)

Figure 4
(*a*) Interactions between $DPLA_2$ and the designed peptide LAIYS. The peptide residues are indicated with a 'P' in parentheses. The critical interactions between Tyr(P) OH and His $N^{\delta 1}$ and Asp $O^{\delta 1}$, including other hydrogen bonds between peptide and protein, are indicated by dotted lines. The figure was drawn with *MOLSCRIPT* (Kraulis, 1991) and *Raster3D* (Merritt & Murphy, 1994). (*b*) *LIGPLOT* (Wallace *et al.*, 1995) showing the schematic representation of the interactions between the peptide LAIYS and protein molecule. (*c*) *GRASP* (Nicholls *et al.*, 1991) representation of the binding cavity and the hydrophobic channel. The peptide LAIYS is almost completely buried in the pocket. Two key hydrogen bonds involving His48 and Asp49 of the protein with peptide Tyr OH are also indicated by dotted lines.

suitable for the binding of the peptide, while that of *B* is unsuitable for binding. As the inhibitor molecule diffuses into the hydrophobic channel, it is expected to interact with its constituents, including the residues of the active site. As seen from Table 3, the binding of peptide LAIYS is stabilized by a number of hydrogen bonds formed between the inhibitor and the enzyme. It also forms a number of hydrophobic interactions with the residues of the hydrophobic channel (data not shown). Hereafter, peptide residues will be indicated with a letter P in parentheses to distinguish them from protein residues. The most significant interactions are observed involving Tyr(P) OH with Asp49 $O^{\delta1}$ and His48 $N^{\delta1}$ of the active site. Similar interactions were also observed in the complexes of $DPLA_2$ with natural inhibitors (Chandra *et al.*, 2002*a*,*b*). These

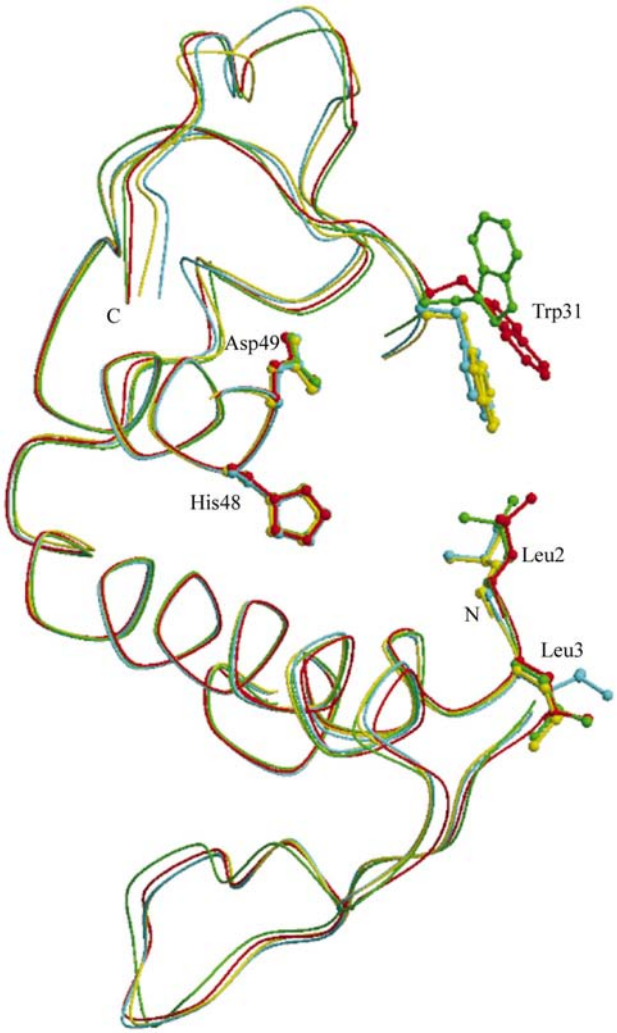

Figure 5
Positioning of Trp31 vis-à-vis the hydrophobic channel: molecule *B* in the native structure of $DPLA_2$ (yellow), molecule *B* in the present complex (blue), molecule *A* in the present complex (red) and molecule *A* in the native structure (green). The distances between the two nearest atoms of Leu2 and Trp31 from two opposite walls of the hydrophobic channel in molecule *A* of native structure is approximately 8.3 and 5.3 Å in the present complex, while in molecule *B* for both native and complex structures these are 4.5 Å. In this complex Trp31 has moved closer to Leu2 after binding to the peptide.

Table 3
Hydrogen-bonded interactions between PLA_2 and the designed peptide Leu-Ala-Ile-Tyr-Ser.

Peptide	Protein	Distance (Å)
Leu1 O	Leu3 N	3.19
Leu1 N	Wat6 OH	3.07
Leu1 N	Wat7 OH	2.87
Ala2 O	Gly6 N	2.84
Tyr4 OH	His48 $N^{\delta1}$	2.98
Tyr4 OH	Wat16 OH	3.29
Tyr4 OH	Asp49 $O^{\delta1}$	2.87
Tyr4 O	Wat16 OH	2.77
Ser5 O^{γ}	Trp31 $N^{\varepsilon1}$	2.63

interactions have displaced a catalytically important water molecule that existed between His48 and Asp49 in the native $DPLA_2$ structures and hence greatly influence the catalytic mechanism in PLA_2 enzymes (Scott *et al.*, 1990). Furthermore, the peptide also forms hydrogen bonds involving Ser(P) O^{γ} with Trp31 $N^{\varepsilon1}$, Tyr(P) O with OW1, Ala(P) O with OW209 and the N-terminal NH_2(P) with Leu3 O (Figs. 4*a* and 4*b*). It also forms a number of strong hydrophobic interactions involving Ile(P) with Phe5 and Phe106, Ala(P) with Ile19 and Leu(P) with Leu10, thus completely filling the hydrophobic channel (Fig. 4*c*). The observed interactions in the present complex are distinct but comparable to those observed in other inhibitors and provide a unique stabilizing effect. These data clearly indicate the key role of the OH group of Tyr(P), giving an important guideline for the design of inhibitors. These observations also indicate a flexibility in the usage of hydrophobic residues for the effective design of PLA_2 inhibitors.

3.5. Comparison of the structure of $DPLA_2$ in the present complex with that in the native state

Although peptide LAIYS binds to molecule *A* at the interface, the nature of the association between the two molecules is not altered. The interactions observed between molecules *A* and *B* in the present complex are identical to those obtained in the native structure (Chandra *et al.*, 2001). Furthermore, the conformations of molecule *B* in the two structures were found to be exactly the same, with a root-mean-square (r.m.s.) shift of 0.3 Å, while those of *A* show an overall similar r.m.s. shift of 0.4 Å, but with a significant variation in the orientation of Trp31. In the native structure, Trp31 of molecule *A* is far removed from the nearest side chain of Leu2, having a shortest distance of 8.3 Å between Trp31 $C^{\zeta2}$ and Leu2 $C^{\delta2}$. The corresponding distance in the complex has reduced to 5.3 Å because of an interaction between Ser(P) O^{γ} and Trp31 $N^{\varepsilon1}$ (Fig. 5).

4. Conclusions

The present structure reconfirms that $DPLA_2$ forms a dimer both in solution as well as in the crystalline state. In fact, the two $DPLA_2$ molecules are always in contact with each other

and dissociate only upon binding to the membrane-like substrates. It is noteworthy that the association induces significant differences in the orientations of Trp31 of the two molecules. While the orientation of Trp31 in molecule *A* is suitable for ligand binding, it is largely unsuitable in molecule *B* owing to narrowing of the mouth of the hydrophobic channel and can only be induced to bind by aggregated ligands such as membrane phospholipids. It further endorses the characteristic behaviour of PLA_2 enzymes in which they show a higher activity towards aggregated substrates (Yuan *et al.*, 1990). It may be noted that PLA_2 enzymes of snake-venom origin have been often found in multimeric forms in which their activities are regulated by the manner of subunit association. In the process of multimerization the access to active-site residues may sometimes be blocked, whereas at other times it might induce changes in the conformation so as to make it unsuitable for simple binding and might need a strong ligand to induce a suitable structure for binding. However, both these aspects enhance enzyme stability, while the activity might be correspondingly reduced. Sometimes only one stabilizing effect is present, while at other times the opposite effect is observed. In the present case both of the above components are present, in which the conformationally suitable site is located at the interface of the two molecules which is physically inaccessible to large substrates, while the exposed binding site adopts an unfavourable conformation. This means that the natural substrates such as membrane phospholipids will be required to dissociate the two molecules to be able to bind to the site residing at the interface and will have to induce a suitable conformation in the exposed site before binding to it. Both these effects will make the activity lower than that of the correctly oriented monomeric forms. It may be mentioned here that the $DPLA_2$ has a comparatively lower activity and higher stability with respect to other PLA_2 enzymes (Kasturi & Gowda, 1989; Kini, 1997; Jayanthi *et al.*, 1989).

Since the design of the present peptide LAIYS is based on the rationality of structural and chemical complementarity to the binding site of the enzyme $DPLA_2$, it fits according to the lock-and-key principle. The designed peptide, however, lacks the capability of inducing a conformational change in molecule *B*, in which the entry to the binding site is blocked by Trp31 and hence fails to interact with it, thus producing an inhibition to the extent of 50% only. On the other hand, the aggregated substrates such as membrane phospholipids act as inducers of suitable orientation of Trp31 in the enzyme, thus leading to the principle of the handshake mechanism. Finally, it can be concluded from the above observations that the peptide LAIYS has a higher affinity for the correctly formed binding site in PLA_2, while an aggregated substrate possesses a higher potential for inducing a suitable conformation for binding. In view of this, the present peptide LAIYS appears to be an excellent inhibitor of correctly formed PLA_2s and can be exploited further for therapeutical applications against inflammation.

The authors thank the Department of Science and Technology for financial assistance. JJ thanks the Council of Scientific and Industrial Research, New Delhi for the award of a fellowship. The authors also acknowledge the support of DST (New Delhi) and DAAD (Bonn) for the Project-based Personnel Exchange Programme 2000 and a grant No. BE 1443/9-1 from DFG (Germany) to CB.

References

Brünger, A. T., Adams, P. D., Clore, G. M., DeLano, W. L., Gros, P., Grosse-Kunstleve, R. W., Jiang, J. S., Kuszewski, J., Nilges, N., Pannu, N. S., Read, R. J., Rice, L. M., Simonson, T. & Warren, G. L. (1998). *Acta Cryst.* D**54**, 905–921.

Chandra, V., Jasti, J., Kaur, P., Srinivasan, A., Betzel, Ch. & Singh, T. P. (2002*a*). *J. Mol. Biol.* **320**, 215–222.

Chandra, V., Jasti, J., Kaur, P., Srinivasan, A., Betzel, Ch. & Singh, T. P. (2002*b*). In the press.

Chandra, V., Kaur, P., Jasti, J., Betzel, Ch. & Singh, T. P. (2001). *Acta Cryst.* D**57**, 1793–1798.

Chandra, V., Kaur, P., Srinivasan, A. & Singh, T. P. (2000). *J. Mol. Biol.* **296**, 1117–1126.

Chandra, V., Nagpal, A., Kaur, P. & Singh, T. P. (1999). *Acta Cryst.* D**55**, 925–926.

Cruickshank, D. W. J. (1999). *Acta Cryst.* D**55**, 583–601.

Dahneke, B. E. (1983). *Measurement of Suspended Particles by Quasi-Elastic Light Scattering*. New York: Wiley.

Jayanthi, G. P., Kasturi, S. & Gowda, T. V. (1989). *Toxicon*, **27**, 875–885.

Jones, T. A., Zou, J., Cowan, S. W. & Kjeldgaard, M. (1991). *Acta Cryst.* A**47**, 110–119.

Kasturi, S. & Gowda, T. V. (1989). *Toxicon*, **27**, 229–237.

Kini, R. M. (1997). Editor. *Venom Phospholipase A_2 Enzymes: Structure, Function and Mechanism*, edited by R. M. Kini, pp. 146–147. Chichester: John Wiley & Sons Ltd.

Kraulis, P. J. (1991). *J. Appl. Cryst.* **24**, 946–950.

Laskowski, R., MacArthur, M., Moss, D. & Thornton, J. (1993). *J. Appl. Cryst.* **26**, 283–290.

Laskowski, R. A., MacArthur, M. W. & Thornton, J. M. (1994). *Proceedings of the CCP4 Study Weekend. From First Map to Final Model*, edited by S. Bailey, R. Hubbard & D. Waller, pp. 149–159. Warrington: Daresbury Laboratory.

Luzzati, V. (1952). *Acta Cryst.* **5**, 802–810.

Merritt, E. A. & Murphy, M. E. P. (1994). *Acta Cryst.* D**50**, 869–873.

Murshudov, G. N. & Dodson, E. J. (1997). *CCP4 Newsl. Protein Crystallogr.* **33**, 31–39.

Nicholls, A., Sharp, K. & Honig, B. (1991). *Proteins*, **11**, 281–296.

Otwinowski, Z. & Minor, W. (1997). *Methods Enzymol.* **176**, 307–326.

Ramachandran, G. N. & Sasisekaran, V. (1968). *Adv. Protein Chem.* **23**, 283–438.

Read, R. J. (1986). *Acta Cryst.* A**42**, 140–149.

Schmitz, K. S. (1990). *An Introduction to Dynamic Light Scattering by Macromolecules*. Boston: Academic Press.

Schulze, T. (1996). MSc thesis. University of Hamburg, Hamburg, Germany.

Scott, D. L., White, S. P., Otwinowski, Z., Yuan, W., Gelb, M. H. & Sigler, P. B. (1990). *Science*, **250**, 1541–1546.

Wallace, A. C., Laskowski, R. A. & Thornton, J. M. (1995). *Protein Eng.* **8**, 127–134.

Wery, J. P., Schevitz, R. W., Clawson, D. K., Bobbitt, J. L., Dow, E. R., Gamboa, G., Goodson, T. Jr, Hermann, R. B., Kramer, R. M. & McClure, D. B. (1991). *Nature (London)*, **352**, 79–82.

Yuan, W., Quinn, D. M., Sigler, P. B. & Gelb, M. H. (1990). *Biochemistry*, **29**, 6082–6094.